

# On the glassy dynamics and the volcano transition of frustrated oscillators

(Dated: April 30, 2024)

## I. INTRODUCTION

Ottino and Strogatz recently published work [1] revisiting a longstanding problem in the theory of coupled oscillators. They propose a model of  $N$  coupled oscillators with frustration,

$$\dot{\theta}_j = \omega_j + J \sum_{k=1}^N A_{jk} \sin(\theta_k - \theta_j), \quad (1)$$

with frequencies  $\omega_j$  sampled from a Lorentzian distribution,  $J$  a variable coupling constant, and  $A$  an adjacency matrix defined by elements

$$A_{jk} = \sum_{m=1}^K (-1)^m u_m^{(j)} u_m^{(k)}/N. \quad (2)$$

Here,  $u_m^{(j)}$  are random vectors with each element independent and equal to  $\pm 1$  with equal probability. Since the signs of the adjacency matrix elements are random, the coupling is both attractive and repulsive, leading to frustration.

The adjacency matrix is formed by  $K$  linearly independent (since each  $u_m$  is random) rank-one updates, and so the rank of the adjacency matrix is  $K$ . For even  $K$ , the diagonal of  $A_{ij}$  is also guaranteed to vanish. Ottino and Strogatz noted an interesting volcano transition for low-rank ( $K \ll \log_2 N$ ) systems. In this case for  $N \gg 1$ , they show that the incoherent state is unstable for  $J > 2$ . For such parameters, clusters emerge, and a low-dimensional Ott-Antonsen reduction suggests that the relaxation to this clustered state will be exponential. They numerically observe this exponential relaxation in the Kuramoto order parameter  $r$  given by

$$re^\Theta = \frac{1}{N} \sum_{j=1}^N e^{i\theta_j}. \quad (3)$$

They note that for large  $K$ , on the other hand, the Ott-Antonsen theory gives a high-dimensional system and the relaxation appears to be algebraic. However, the numerical simulations were limited and the evidence is not entirely clear. The main motivation comes from Daido's model for glassy dynamics in frustrated networks of coupled oscillators [2]. For  $K = N \gg 1$ , the adjacency matrix is well approximated by random matrix elements which are normally distributed (by the central limit theorem), which Daido studied previously. Daido's relation to glassy dynamics was apparently contentious, and Ottino and Strogatz seemed to hope that their variable-rank model could shine a light on the question. However, the problem remains open.

Our main goal here is to apply data-driven methods to shine a light on the high-dimensional glassy dynamics in the large  $K$  and large  $N$  limit. One possibility we have considered is PCA or DMD analyses to try to infer the intrinsic dimensionality. Another approach is to use SINDy on the dynamics of the order parameter to distinguish between the exponential and algebraic relaxation. In the course of these studies, we have implemented efficient numerical integration on the GPU in order to observe the scaling for large  $N$  and  $K$  [3]. Our efficient simulations are capable of exploring systems as large as  $N = 10^6$ , which is three orders of magnitude larger than those considered by Ottino and Strogatz.

In exploring these larger systems, we have also noted subtlety in the glassy decay that could not have been recognized for the previously considered cases with  $N < 10^4$ . In particular, we find that the decay only appears algebraic after an initial period of exponential decay. This onset period increases with increasing  $N$ . The balance between the scaling of the noise floor and the onset period with increasing  $N$  is pertinent for the large  $N$  limit.

## II. ANALYTICAL CONSIDERATIONS

Starting from a state of identical phases  $\theta_i = 0$ , the system is expected to relax to the incoherent state for large  $N$  and  $K$  for which there is no clustering and the oscillator phases are uniformly random and independent. We can analytically predict the finite- $N$  scaling of the order parameter for this incoherent state. In this case, the real and imaginary components of the complex order parameter will be sums of  $N$  independent random variables (sampled

by taking the cosine and sign of a uniform distribution). For large  $N$ , by the central limit theorem, these sums will converge to two independent normal distributions each with variance  $1/2N$ . The magnitude of the order parameter will then be distributed as a Rayleigh distribution with  $\sigma = (2N)^{-1/2}$ , and the mean magnitude of the order parameter is then

$$r_{\text{incoherent}} = \sqrt{\pi/4N}. \quad (4)$$

This is the “noise floor” observed in numerical simulations.

### III. NUMERICAL CONSIDERATIONS

Ottino and Strogatz used a fixed timestep  $dt = 0.01$  with a 4th-order Runge-Kutta method on a CPU. We implement instead an adaptive time-stepping Dormand-Prince with a 5/4 embedding Runge-Kutta method on the GPU (the same method used by the `ode45` in Matlab and the Python `scipy` method `solve_ivp`). The trajectory is sampled at the  $dt = 0.01$  timesteps using a “free” fourth-order polynomial interpolation. We reproduce both the low  $K = 2$  clustered states and the apparent high- $K$  algebraic decay to incoherence for  $N = 5000$  oscillators in Fig. 1(a).

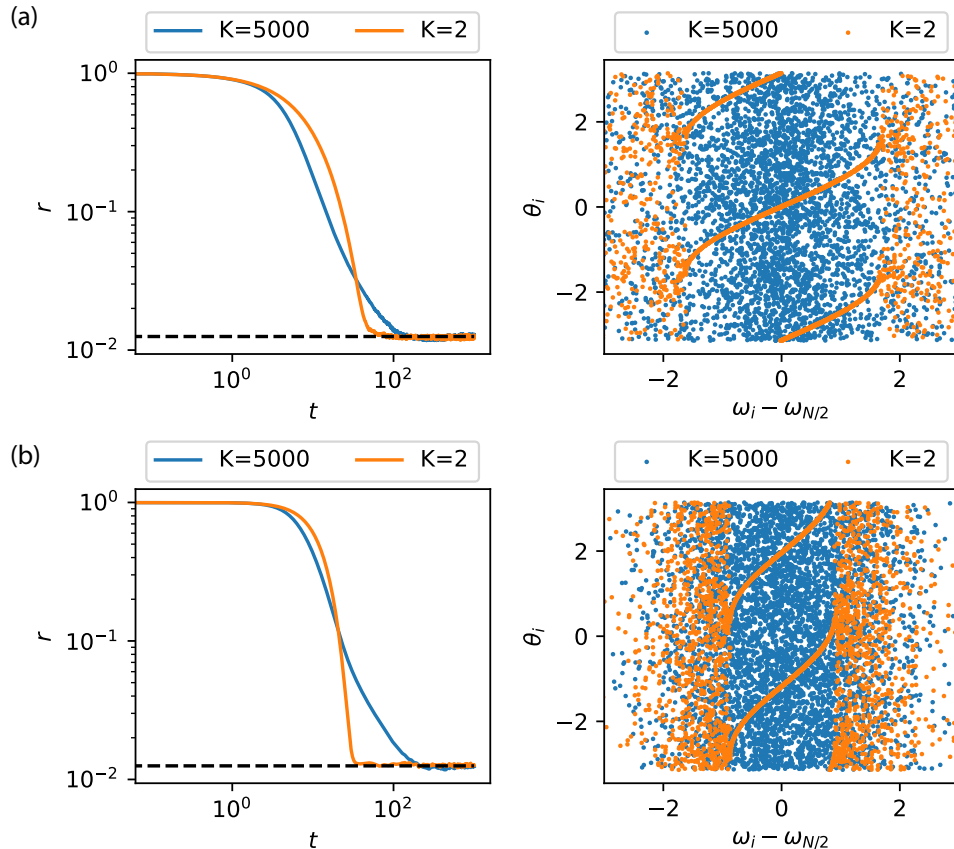


FIG. 1. Volcano clusters for small  $K$  and slow decay to incoherence for large  $K$  for Lorenztian distributed frequencies with  $J = 2$  (a) and normal distributed frequencies with  $J = 1.75$  (b), with  $N = 5000$ . The noise floor from Eq. (4) is shown by the dashed black line. Order parameters are averaged over 750 simulations.

Our first observation is that the fixed time step used by Ottino and Strogatz is not sufficiently small to guarantee an accurate solution for the problem with Lorenztian distributed frequencies, even for the small systems with  $N = 5000$  presented. To control the error well, the timestep should be smaller than  $O(T_m)$  where  $T_m = 2\pi/\omega_M$  is the natural period of the fastest oscillator since otherwise, the contributions to Eq. (1) will oscillate many times between time steps. If the frequencies are distributed with a probability density  $f(\omega)$ , it can be shown that the distribution for the maximum frequency of  $N$  samples is  $Nf(\omega)F(\omega)^{N-1}$ , where  $F$  is the cumulative probability distribution, i.e.  $F'(\omega) = f(\omega)$ . So the expected maximum frequency is  $\omega_M = \int N\omega f(\omega)F(\omega)^{N-1}d\omega$ . For the standard Lorenztian

distribution, this gives  $\omega_M \sim 1.6475N$  asymptotically for large  $N$ , leading to  $T_m = 0.0076$  for  $N = 5000$ . Indeed, our adaptive time step uses  $dt \approx 0.0015$  for  $K = N = 5000$ . This scaling poses a significant challenge to increasing  $N$  with Lorentzian-distributed natural frequencies. On the other hand, as shown in Fig. 1(b), we observe a similar volcano transition for normally distributed natural frequencies in the small  $K$  case, although the analytical Ott-Anstonsen predictions are not applicable and we find that the critical coupling  $J_c$  is smaller than the value of 2 in the Lorentzian case. For the normal distribution, we find a much slower growth with  $\omega_M < \log N$  (I'm sure some asymptotics can be done here as well...). Thus, we opt to use normally distributed natural frequencies instead. In the normally distributed case, the adaptive time step does not become prohibitively small even for  $N$  and  $K$  up to  $10^6$ .

A second consideration for large  $N$  and  $K$  is the memory required to store the adjacency matrix. This requires at least  $N \times K$  bits to store the  $u_m(j) = \pm 1$  values, and, more simply,  $N^2 \times 8$  bytes to store each floating point in the adjacency matrix. Modern graphics cards typically have less than 20 GB of memory available, so this would constrain  $N = K \lesssim 5 \times 10^4$  if we store the entire adjacency matrix during the computation. However, the numerical integration routine itself requires only  $O(N)$  bytes of memory. By careful use of the counter-based Philox64 random number generator, we can efficiently regenerate the numbers at an arbitrary position of a fixed random sequence without storing the entire sequence. Thus, we can recalculate the adjacency elements in each CUDA kernel call only when required, and keep the memory requirements down to  $O(N)$ . Our limitation is then only the time required to integrate the system. In this way, it takes less than ten seconds to integrate  $K = N = 10^4$  oscillators and about two days to integrate  $K = N = 10^6$  oscillators with normally distributed natural frequencies. (Compare this with scipy integration on a CPU, which takes about two minutes for the  $K = N = 10^4$  case).

#### IV. SINDY FITS

We first contrast SINDy fits for  $N = 5000$  and  $K = 2$  or  $K = N$ . We average the order parameter  $r$  over 750 simulations with differing random seeds, and restrict the time interval to the period in which  $5/\sqrt{N} < r < 0.5$ . We use a polynomial library with terms up to order 5, and increase the threshold to eliminate as many terms as possible while achieving good fits. For  $K = 2$ , SINDy discovers a model

$$\dot{r}_{\text{pred}} = -2.258r + 2.238r^2, \quad (5)$$

with the leading order linear term giving rise to the expected exponential decay. For  $K = N$ , we find a model

$$\dot{r}_{\text{pred}} = -10.449r^2 + 26.487r^3 + -22.338r^4. \quad (6)$$

Interestingly, the linear term is eliminated, and the leading order decay is expected to be algebraic. For both fits, the R2 score is greater than 0.99, and the comparison between the predicted  $\dot{r}_{\text{pred}}$  and the actual value  $\dot{r}$  is shown in Fig. 2.

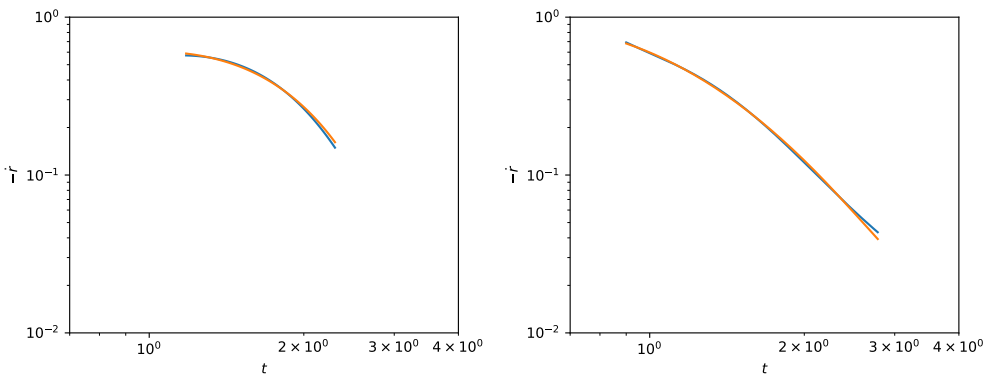


FIG. 2. SINDy predictions (orange lines) and actual time derivatives (blue lines) for the model in Eq. (5) with  $K = 2$  (a) and the model in Eq. (6) with  $K = N = 5000$  (b).

## V. LARGE $N$ SCALING

Next, we consider the transition between the exponential and algebraic decay as  $K$  and  $N$  increase. Figure 3 shows our results for cases with  $N \in (10^4, 2 \times 10^4, 10^5, 2 \times 10^5)$ . We see that for intermediate  $K/N$ , there is a change from exponential to algebraic decay around  $t = 5$ , with the time of onset of the transition increasing modestly with increasing  $N$ . The rate of the algebraic decay decreases with increasing  $N$ , because the difference between the  $O(N^{-1/2})$  noise floor in Eq. (4) and the values of  $r$  at the transition time become increasingly small. Thus, the purported algebraic decay appears to be confined to an increasingly short period as  $N$  increases, but the rate of decay is also increasingly slow. The limiting behavior as  $N \rightarrow \infty$  is still unclear, but the simulations suggest a more complex asymptotics than previously suggested. (We may want to consider fixed  $K = c \log(N)$  to try to fix the time of the onset of the transition.)

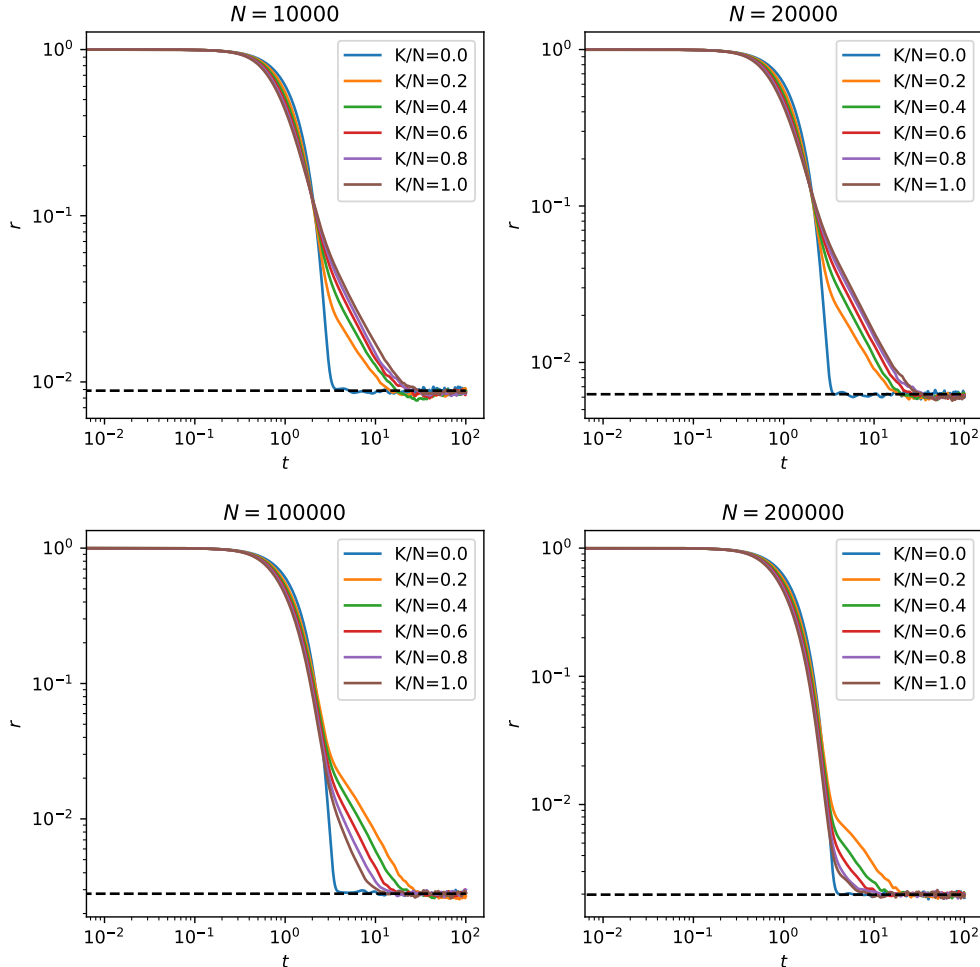


FIG. 3. Order parameter averaged over 500 simulations vs time for various values of  $N$  and  $K$ .

## VI. KOOPMAN AND DMD ANALYSIS

The flow induced by Eq. (1) on the torus  $\mathcal{T}^N$  is generated by vector field

$$\mathbf{v} = \sum_i \left( \omega_i + J \sum_j A_{ij} \sin(\theta_j - \theta_i) \right) \mathbf{v}_i, \quad (7)$$

where  $\mathbf{v}_i = \frac{\partial}{\partial \theta_i}$  is the unit vector corresponding to the usual angle coordinate  $\theta_i$  on  $\mathcal{T}^N$ . The nonlinear dynamics in Eqs. (1) can be equivalently described by the linear Liouville-von Neuman equation for a probability density  $\rho : \mathcal{T}^N \rightarrow \mathbb{R}$ ,

$$\frac{\partial \rho}{\partial t} = \mathcal{L}_{\mathbf{v}}^\dagger(\rho) \equiv - \sum_i \frac{\partial}{\partial \theta_i} \left[ \left( \omega_i + J \sum_j A_{ij} \sin(\theta_j - \theta_i) \right) \rho \right], \quad (8)$$

or by the adjoint equation describing the infinitesimal flow of measurements quantities  $g : \mathcal{T}^N \rightarrow \mathbb{R}$ ,

$$\frac{\partial g}{\partial t} = \mathcal{L}_{\mathbf{v}}(g) \equiv \sum_i \left( \omega_i + J \sum_j A_{ij} \sin(\theta_j - \theta_i) \right) \frac{\partial g}{\partial \theta_i}. \quad (9)$$

The literature often considers the exponentiated forms, corresponding to the Koopman operator  $\mathcal{K}^\tau \equiv e^{\tau \mathcal{L}_{\mathbf{v}}}$  and the Perron-Frobenius operator  $\mathcal{P}^\tau \equiv e^{\tau \mathcal{L}_{\mathbf{v}}^\dagger}$ , but the infinitesimal forms are simple and convenient here. It is clear that any Koopman eigenfunction  $\mathcal{K}^\tau[g] = \lambda g$  is also a Lie generator eigenfunction  $\mathcal{L}_{\mathbf{v}}[g] = \mu g$  and vice versa, and the eigenvalues are related by  $\lambda = e^{\mu \tau}$ .

It is natural to consider the Sobolov spaces and embeddings here since the operator  $\mathcal{L}_{\mathbf{v}}$  involves only first-order derivatives and the domain  $\mathcal{T}^N$  is compact. I'll be a little less formal...consider first the  $L^2$  functions, and note that we can use the Fourier basis to express functions as infinite-dimensional vectors of Fourier coefficients. That is, equate the  $L^2$  function  $g(\theta) = \sum_{\mu \in \mathbb{Z}^N} g_\mu e^{i \sum_i \mu_i \theta_i}$  with the  $\ell^2$  coefficients  $g_\mu$ , where  $\mu \in \mathbb{Z}^N$  spans over all lists of  $N$  integers and  $i \equiv \sqrt{-1}$ . Then, it is easy to show that the Lie generator  $\mathcal{L}_{\mathbf{v}}$  acts on  $g_\mu$  as a matrix  $\sum_{\nu \in \mathbb{Z}^N} L_{\mu\nu} g_\nu$  where

$$L_{\mu\nu} = i \sum_i \omega_i \nu_i \delta_\mu^\nu + J \sum_{ij} A_{ij} \nu_i (\delta_\mu^{\nu + \mathbf{e}_j - \mathbf{e}_i} - \delta_\mu^{\nu - \mathbf{e}_j + \mathbf{e}_i}) / 2. \quad (10)$$

Here,  $\mathbf{e}_j$  is the vector with a unit entry in the  $j$ th element and a zero in all others and  $\delta_\mu^\nu = \prod_i \delta_{\mu_i}^{\nu_i}$  is the product of the Kronecker delta over all indices. Note that for  $J = 0$ , the matrix  $L_{\mu\nu}$  is diagonal, and indeed the Fourier basis elements  $\hat{g}_\mu(\theta) = e^{i \sum_i \mu_i \theta_i}$  are Koopman eigenfunctions with (generator) eigenvalues  $\mu = i \sum_i \mu_i \omega_i$ . We can then consider the case of small  $J \ll 1$  as a perturbation to the diagonal matrix and ask what the perturbed eigenfunctions and eigenvalues are. **Questions:** In the limit of large  $N$ , is the perturbation compact? The unperturbed eigenvalues accumulate continuously on the real line, so do they form the essential spectrum that remains invariant under compact perturbations by Weyl's criterion?

Although the case of large perturbations is more difficult, the DMD results in Fig. 4 show a data-driven estimate for the Koopman eigenvalues and eigenfunctions. We observe that many eigenvalues stay close to the imaginary axis, but isolated cases seem to acquire a negative real component. The eigenvalue density on the imaginary axis appears to concentrate toward zero in the glassy case.

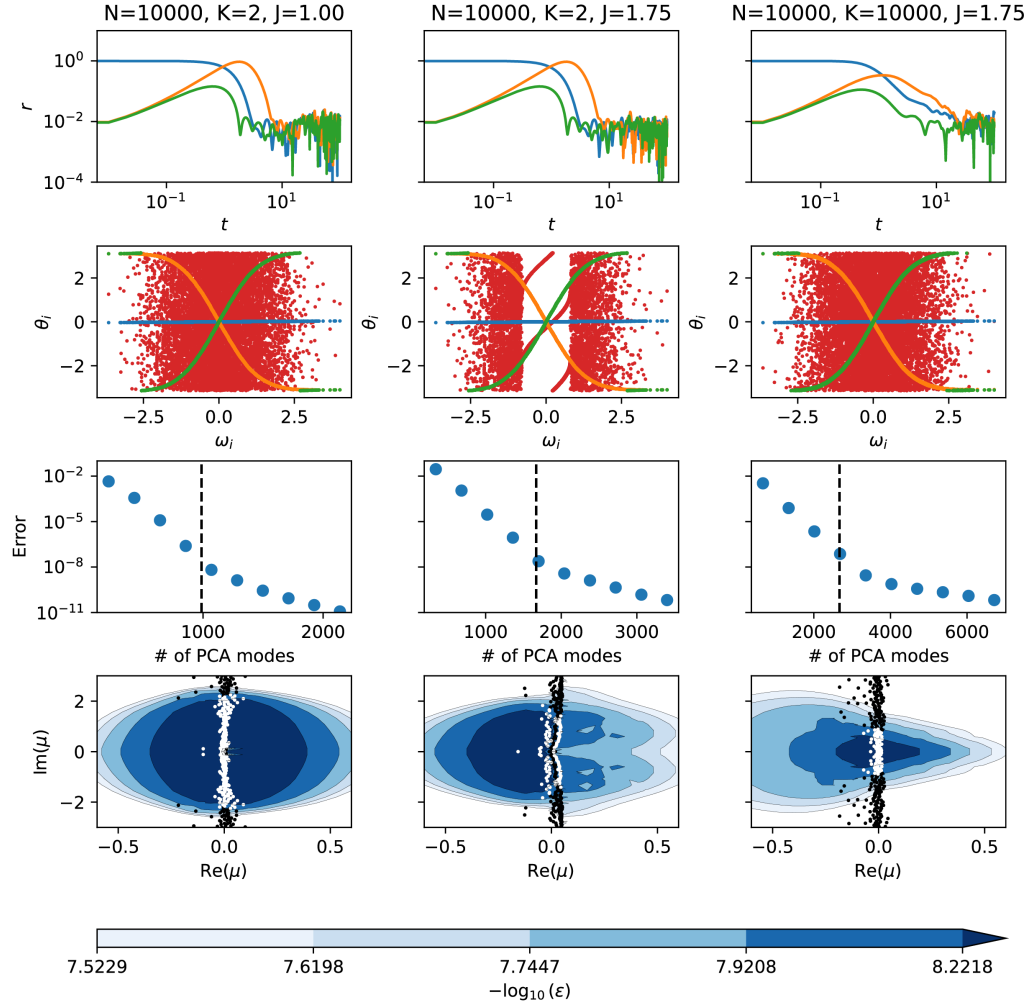


FIG. 4. Residual DMD eigenvalues and pseudospectrum for  $N = 10000$  oscillators,  $K = 2$  and  $J = 1$  (first column) corresponding to an exponential relation to incoherence,  $K = 2$  and  $J = 1.75$  (second column) corresponding to exponential relation to a volcano clustered state and  $K = 10000$  and  $J = 1.75$  (third column) corresponding to algebraic relation related to the oscillator glass.

- 
- [1] Ottino-Löffler, Bertrand, and Steven H. Strogatz. "Volcano transition in a solvable model of frustrated oscillators." *Physical review letters* 120, no. 26 (2018): 264102.
  - [2] Daido, Hiroaki. "Quasientrainment and slow relaxation in a population of oscillators with random and frustrated interactions." *Physical review letters* 68, no. 7 (1992): 1073.
  - [3] See our github repository for source code and data: <https://github.com/znicolaou/kuramoto>.